Available online at www.sciencedirect.com
SCIENCE DIRECT®
Journal of Power Sources 119–121 (2003) 150–155
JOURNAL OF POWER SOURCES
www.elsevier.com/locate/jpowsour

Comparative study of $Li(Ni_{0.5-x}Mn_{0.5-x}M_{2x}')O_2$ ($M' = Mg, Al, Co, Ni, Ti$; $x = 0, 0.025$) cathode materials for rechargeable lithium batteries☆

S.-H. Kang*, K. Amine

Electrochemical Technology Program, Chemical Technology Division, Argonne National Laboratory, Argonne, IL 60439, USA

Abstract

We have investigated the effect of dopants on the electrochemical and thermal properties of layered $Li(Ni_{0.5-x}Mn_{0.5-x}M_{2x}')$ materials ($M' = Mg, Al, Co, Ni, Ti$; $x = 0, 0.025$) that were prepared using a manganese–nickel hydroxide precursor. $Li(Ni_{0.5}Mn_{0.5})O_2$ exhibited discharge capacities of ca. 120 and 150 mAh/g at 2.8–4.3 and 2.8–4.6 V, respectively, with slight capacity fades; the addition of 5 mol% Al, Co, Ni, and Ti increased discharge capacity by 10–30% and improved capacity retention. X-ray photoelectron spectroscopy data suggested that Ni and Mn exist as Ni^{2+} and Mn^{4+} so that only Ni is electrochemically active in the layered structure. Differential scanning calorimetry (DSC) data showed that exothermic reactions of $Li_y(Ni_{0.5-x}Mn_{0.5-x}M_{2x}')O_2$ charged to 4.3 V versus Li started at higher temperatures (270–290 °C) than $LiNiO_2$-based cathode materials (e.g. 200 °C for $LiNi_{0.8}Co_{0.2}O_2$), which indicates that the thermal stability of $Li(Ni_{0.5-x}Mn_{0.5-x}M_{2x}')$ is superior to that of $LiNiO_2$-based cathode materials.

Keywords: Lithium-ion rechargeable battery; Cathode materials; Lithium manganese nickel oxides; Layered structure

1. Introduction

According to recent reports by Ohzuku and Makimura [1] and Lu et al. [2], layered $Li(Ni_{0.5}Mn_{0.5})O_2$ is an attractive cathode material for rechargeable lithium batteries in several aspects. $Li(Ni_{0.5}Mn_{0.5})O_2$ does not transform to spinel structure during electrochemical cycling and shows no sign of structural degradation due to multiphase reactions at higher voltages (>4.3 V), which are major drawbacks of $LiMnO_2$ and $LiNiO_2$, respectively. Furthermore, because the Mn content is higher and the Ni content lower than in $LiNiO_2$, $Li(Ni_{0.5}Mn_{0.5})O_2$ is cost-effective and less toxic, and improved thermal safety is anticipated.

However, further improvement is needed before the material is suitable for practical uses such as high-energy and/or high-power applications; $Li(Ni_{0.5}Mn_{0.5})O_2$ exhibits rather low capacity in normal operating voltage windows (e.g. 2.8–4.3 V) compared with $LiNiO_2$-based materials, and our preliminary studies revealed that it showed rather high impedance for high-power applications such as hybrid electric vehicles (HEVs).

In this work, layered $Li(Ni_{0.5}Mn_{0.5})O_2$ materials with various dopants were prepared using a Mn–Ni mixed hydroxide precursor. The effects of dopants on cycling performance, impedance, and thermal reactivity of these materials were investigated. Oxidation states of Ni and Mn in the structure were examined by X-ray photoelectron spectroscopy (XPS).

2. Experimental

$Li(Ni_{0.5-x}Mn_{0.5-x}M_{2x}')$ ($M' = Mg, Al, Co, Ni, Ti$; $x = 0, 0.025$) was prepared using appropriate amounts of $LiOH{\cdot}H_2O$, manganese–nickel hydroxide (OMG, Mn:Ni = 1:1), $Mg(OH)_2$, $Al(OH)_3$, $Co(OH)_2$, $Ni(OH)_2$, and TiO_2. The starting powders were mixed in acetone using zirconia balls; the mixed powders were calcined at 600 °C for 16 h and then at 1000 °C for 15 h in air. Phase purity of the synthesized materials was established by powder X-ray diffraction (XRD) using Cu Kα radiation.

Electrochemical properties of the synthesized materials were examined using galvanostatic cycling and cyclic voltammetry with coin cells at room temperature. The cathode mixtures consisted of 82 wt.% metal oxide powder, 10 wt.%

☆The submitted manuscript has been created by the University of Chicago as Operator of Argonne National Laboratory ('Argonne') under Contract no. W-31-109-ENG-38 with the US Department of Energy. The US Government retains for itself, and others acting on its behalf, a paid-up, nonexclusive, irrevocable worldwide license in said article to reproduce, prepare derivative works, distribute copies to the public, and perform publicly and display publicly, by or on behalf of the Government.

* Corresponding author. Tel.: +1-630-252-6772; fax: +1-630-252-4176.
E-mail address: kangs@cmt.anl.gov (S.-H. Kang).

0378-7753/03/$ – see front matter © 2003 Elsevier Science B.V. All rights reserved.
doi:10.1016/S0378-7753(03)00145-9

carbon, and 8 wt.% polyvinylidene difluoride (PVDF) binder on aluminum foil. The negative electrode was either metallic lithium or graphite on copper foil. The electrolyte was 1 M $LiPF_6$ in a 1:1 mixture of ethylene carbonate (EC)/diethyl carbonate (DEC); the separator was Celgard 2500.

Differential scanning calorimetry experiments were conducted on $Li_y(Ni_{0.5-x}Mn_{0.5-x}M_{2x}')O_2$ samples charged to 4.3 V (versus metallic Li). The data were acquired using a Perkin-Elmer Pyris 1 differential scanning calorimeter (DSC) at a scan rate of 10 °C/min in the temperature range of 50–350 °C. Commercial (Perkin-Elmer), hermetically sealed crucibles that contained the charged cathode materials (typically ca. 1 mg) and 3 μl of electrolyte were used for all samples.

3. Results and discussion

The powder XRD patterns of $Li(Ni_{0.5-x}Mn_{0.5-x}M_{2x}')$ ($M' = Mg$, Al, Co, Ni, Ti; $x = 0$, 0.025) are shown in Fig. 1. All the materials except $M' = Mg$, showed XRD patterns of well-developed layered materials with $R\bar{3}m$ symmetry.

The discharge curves of $Li/Li(Ni_{0.5-x}Mn_{0.5-x}M_{2x}')$ ($M' = Mg$, Al, Co, Ni, Ti; $x = 0$, 0.025) cells cycled galvanostatically at 2.8–4.3 and 2.8–4.6 V are shown in Figs. 2 and 3, respectively; corresponding discharge capacities are given in Fig. 4. Figs. 2–4 show that all of the dopants except Mg increased discharge capacity by 10–30% and improved cycling stability.

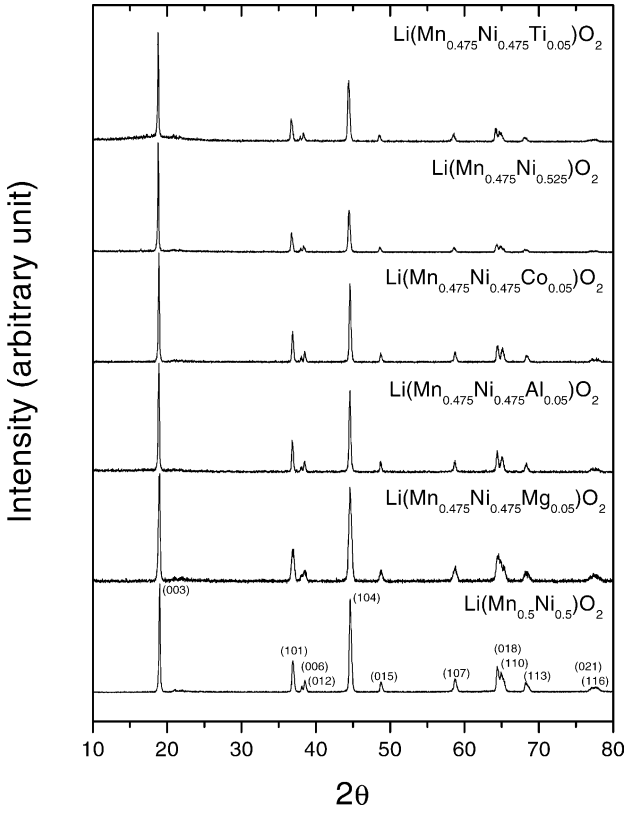

Fig. 1. Powder XRD patterns of $Li(Ni_{0.5-x}Mn_{0.5-x}M_{2x}')$ ($M' = Mg$, Al, Co, Ni, Ti; $x = 0$, 0.025).

The cyclic voltammogram (CV) of $Li/Li(Ni_{0.5}Mn_{0.5})O_2$ cell is shown in Fig. 5. Upon charging, $Li(Ni_{0.5}Mn_{0.5})O_2$ shows a major peak centered at ca. 4.0 V versus Li^+/Li and a small, broad peak at ca. 4.4 V versus Li^+/Li, which is quite different from that of $LiNiO_2$ that shows three sharp redox peaks due to three distinct phase transitions [3]. The CVs of other materials are similar to that of $Li(Ni_{0.5}Mn_{0.5})O_2$. It is noted that no redox-reaction peaks are observed near 3 V in the CV. According to Paulsen et al. [4], Mn^{3+}/Mn^{4+} redox reactions occur at about 2.9 V versus Li^+/Li in layer-structured $Li_{2/3}(Ni_{1/3}Mn_{2/3})O_2$. Therefore, the absence of the redox-reaction peaks in the 3 V region indicates that Mn ions are electrochemically inactive and, therefore, presumed to be present as Mn^{4+}. In a purely ionic scenario, Ni ions must exist as Ni^{2+} in $Li(Ni_{0.5}Mn_{0.5})O_2$ to maintain charge neutrality. Correspondingly, the peaks centered at ~4 V in the CV are attributed to the redox reactions of Ni^{2+}/Ni^{3+} and/or Ni^{2+}/Ni^{4+}, as was speculated by Lu et al. [2].

To determine the oxidation states of Ni and Mn in the layered materials, we conducted XPS experiments on $Li(Ni_{0.5}Mn_{0.5})O_2$; the electron-binding energies of Ni and Mn of $Li(Ni_{0.5}Mn_{0.5})O_2$ and reference compounds are listed in Table 1. In $Li(Ni_{0.5}Mn_{0.5})O_2$, the Ni $2p_{3/2}$ peak is at 854.3 eV, which is similar to the binding energy of Ni^{2+} in NiO. The Mn $2p_{3/2}$ peak is at 642.1 eV, which is closer to the value measured for Mn^{4+} in λ-MnO_2 than for Mn^{3+} in $Li_2Mn_2O_4$. Furthermore, the Mn 3p peak at 49.8 eV is similar to that measured for Mn^{4+} in λ-MnO_2. These data suggest that Ni and Mn ions are present as Ni^{2+} and Mn^{4+}, respectively. However, other experiments such as X-ray absorption spectroscopy (XAS) are necessary to determine conclusively the elemental oxidation states in the bulk sample.

Differential scanning calorimetry profiles of $Li_y(Ni_{0.5-x}Mn_{0.5-x}M_{2x}')O_2$ samples charged to 4.3 V versus Li in $Li/Li(Ni_{0.5-x}Mn_{0.5-x}M_{2x}')$ cells are shown in Fig. 6; data from $Li_y(Ni_{0.80}Co_{0.20})O_2$ charged to 4.2 V [7] are also shown for comparison. $Li_y(Ni_{0.5-x}Mn_{0.5-x}M_{2x}')O_2$ exhibited simple DSC curves with onset temperatures of exothermic reactions higher than 270 °C, whereas $Li_y(Ni_{0.80}Co_{0.20})O_2$ showed

Table 1
Electron binding energies of $Li(Ni_{0.5}Mn_{0.5})O_2$ and reference oxides

Compound	Binding energy (eV)			Reference
	Mn $2p_{3/2}$	Mn 3p	Ni $2p_{3/2}$	
$Li(Ni_{0.5}Mn_{0.5})O_2$	642.1	49.8	854.3	This work
NiO			854.1	This work
Ni_2O_3			855.2	This work
$LiNiO_2$			855.4	[5]
$Li_2Mn_2O_4$	641.4	48.5		[6]
λ-MnO_2	642.4	49.7		[6]

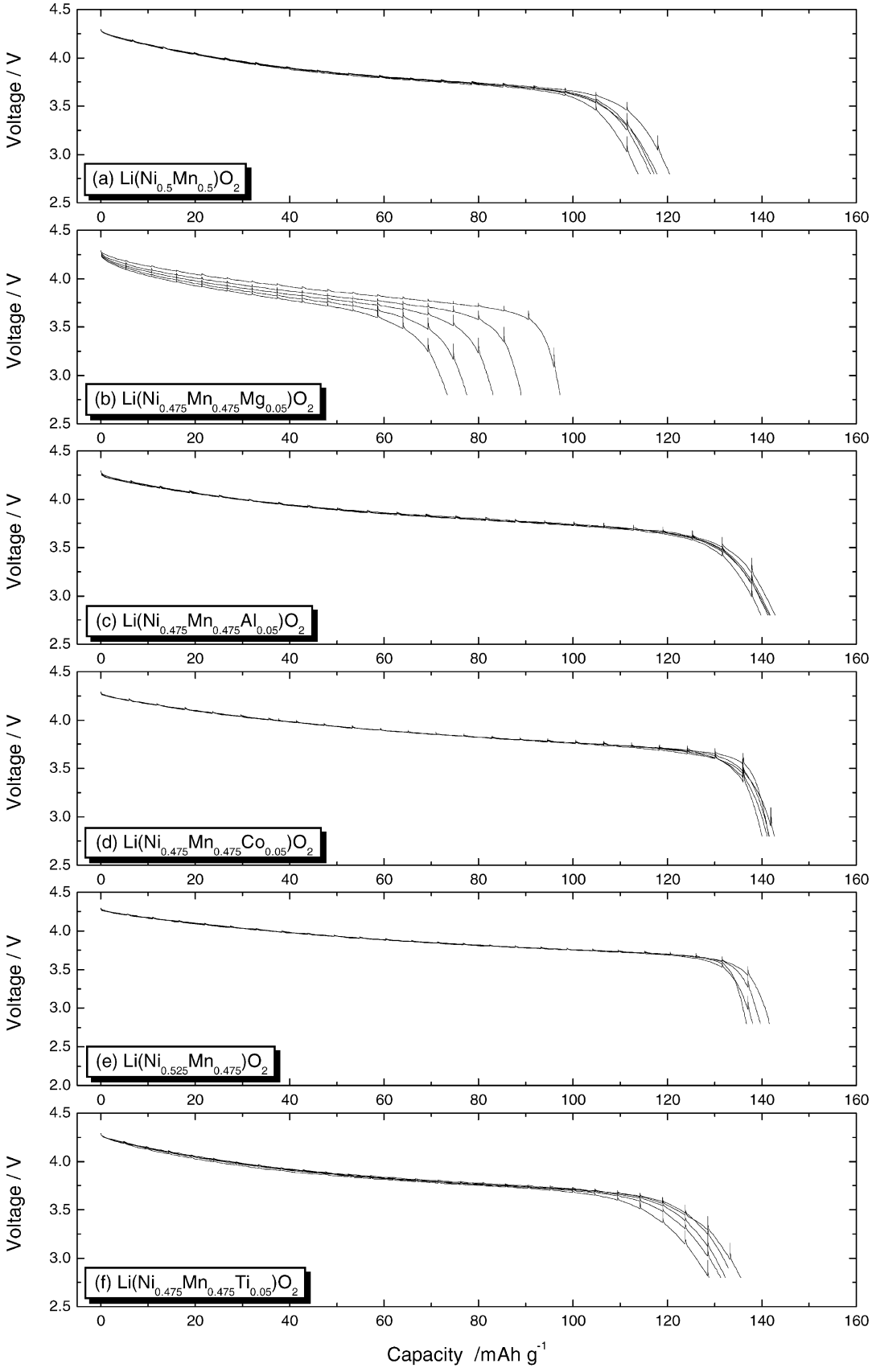

Fig. 2. Discharge curves of Li/Li($Ni_{0.5-x}Mn_{0.5-x}M_{2x}'$) (M′ = Mg, Al, Co, Ni, Ti; $x = 0$, 0.025) cells in the voltage range of 2.8–4.3 V at a current density of 0.1 mA/cm^2.

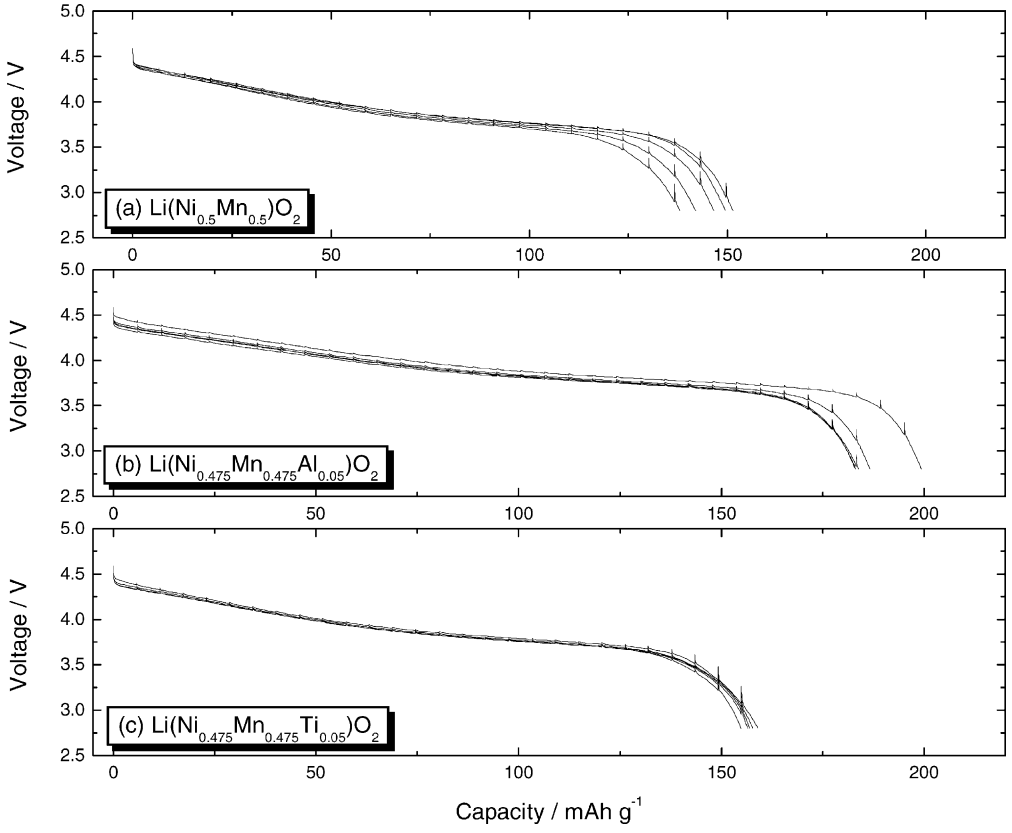

Fig. 3. Discharge curves of Li/Li($Ni_{0.5-x}Mn_{0.5-x}M_{2x}'$) (M′ = Al, Ti; $x = 0,\ 0.025$) cells in the voltage range of 2.8–4.6 V at a current density of 0.1 mA/cm^2.

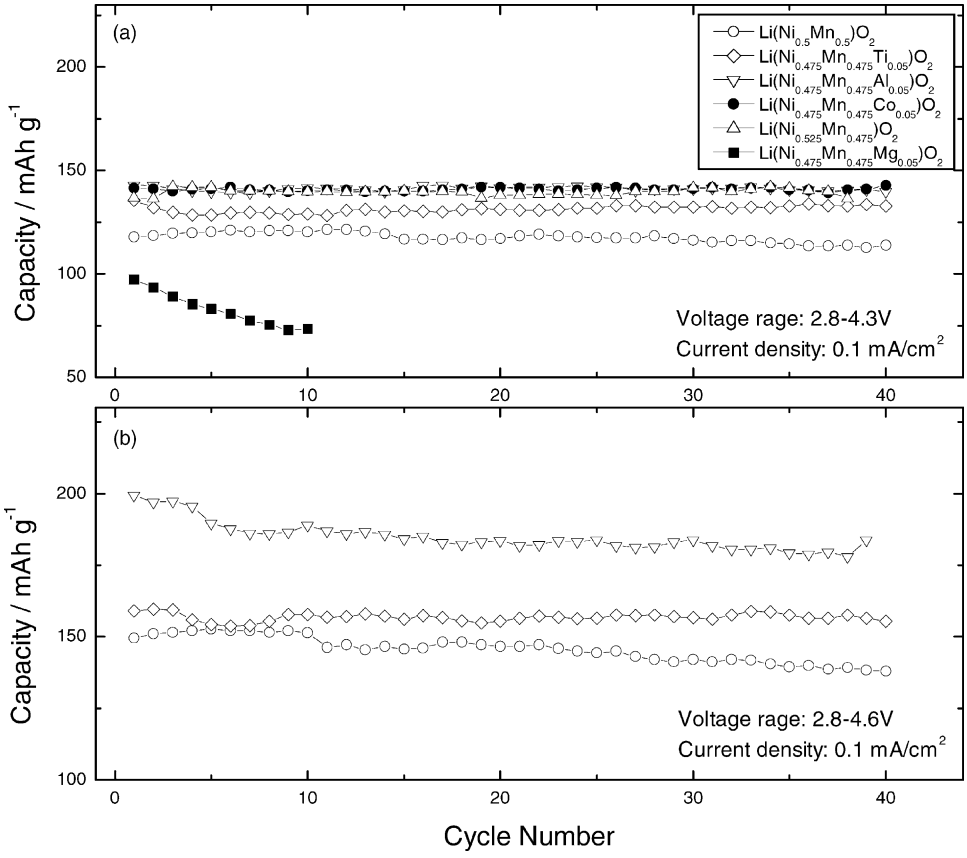

Fig. 4. Discharge capacities of Li($Ni_{0.5-x}Mn_{0.5-x}M_{2x}'$) (M′ = Mg, Al, Co, Ni, Ti; $x = 0,\ 0.025$) in the voltage range of (a) 2.8–4.3 V and (b) 2.8–4.6 V at a current density of 0.1 mA/cm^2.

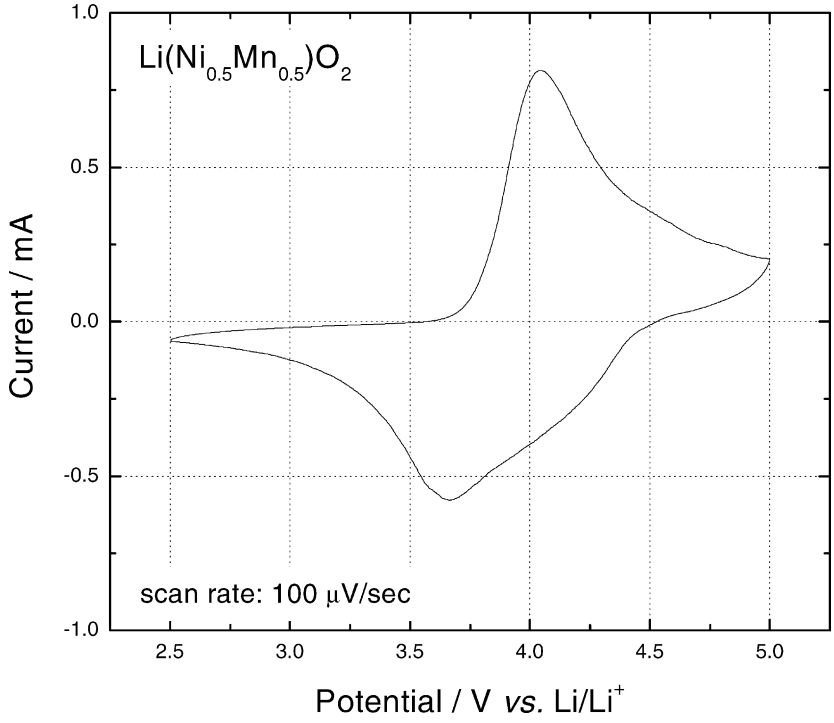

Fig. 5. Cyclic voltammogram of $Li(Ni_{0.5}Mn_{0.5})O_2$ at a sweep rate of 100 μV/s.

three distinct exothermic peaks, with an onset temperature of 200 °C. Total heat associated with the exothermic reactions is comparable to $[Li_y(Ni_{0.5}Mn_{0.5})O_2$, $Li_y(Ni_{0.475}Mn_{0.475}Co_{0.05})O_2]$ or much smaller $[Li_y(Ni_{0.475}Mn_{0.475}Al_{0.05})O_2]$ than that of $Li_y(Ni_{0.80}Co_{0.20})O_2$. Consequently, $Li(Ni_{0.5-x}Mn_{0.5-x}M_{2x}')$ materials have better thermal safety characteristics than $LiNiO_2$-based cathode materials, as shown in Fig. 6 and described by Gao et al. [8].

Area specific impedance (ASI) is directly related to the power capability of a battery and it should be lower than 35 Ω cm^2 to meet the partnership for a new generation of vehicles (PNGV) requirement for the battery to power an HEV [9]. Fig. 7 shows ASI as a function of state of charge (SOC) measured with $C/Li(Ni_{0.5-x}Mn_{0.5-x}M_{2x}')$ ($M' = Co$, Al, Ti; $x = 0$, 0.025) cells. The ASI was determined by $(A\Delta V)/I$, where A is the cross-sectional area, ΔV the voltage variation during current interruption for 30 s at each SOC, and I the current applied during the galvanostatic cycling. The $C/Li(Ni_{0.5}Mn_{0.5})O_2$ cell exhibited an ASI value of 64 Ω cm^2 at 40–60% SOC, which is higher than the PNGV requirement. The $C/Li(Ni_{0.475}Mn_{0.475}Ti_{0.05})O_2$ and $C/Li(Ni_{0.475}Mn_{0.475}Al_{0.05})O_2$ cells showed similar (62 Ω cm^2) and higher (99 Ω cm^2) ASI values, respectively, whereas $C/Li(Ni_{0.475}Mn_{0.475}Co_{0.05})O_2$ showed a lower (47 Ω cm^2) ASI value. The decrease of ASI values with the 5 mol% Co-doping is partly attributed to the enhancement of electrical conductivity of the material; preliminary studies revealed that the electrical conductivity increased by 2 orders of magnitude with 5 mol% Co-doping [2.5×10^{-6} and 2.3×10^{-4} Ω^{-1} cm^{-1} for $Li(Ni_{0.5}Mn_{0.5})O_2$ and $Li(Ni_{0.475}Mn_{0.475}Co_{0.05})O_2$, respectively]. Various efforts are being made to lower the ASI values below 35 Ω cm^2 through optimization of various factors, such as nature and content of doping elements, size and morphology of oxide powders, and the quantity of carbon and binder in the cathode.

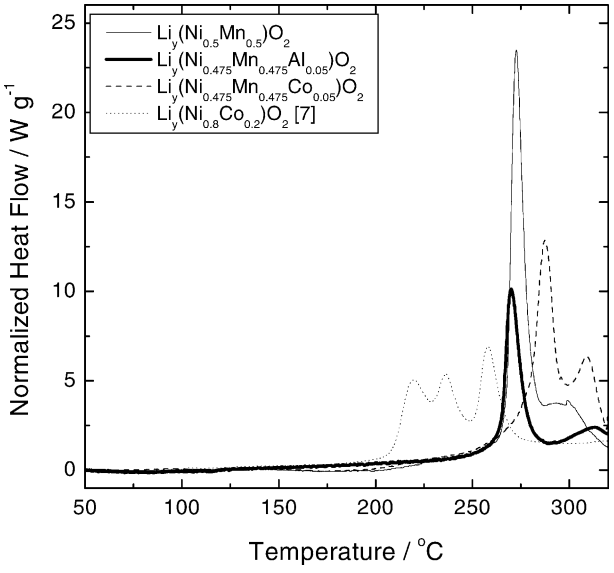

Fig. 6. Differential scanning calorimetry (DSC) profile (10 °C/min) of (a) $Li_y(Ni_{0.5}Mn_{0.5})O_2$, (b) $Li_y(Ni_{0.475}Mn_{0.475}Co_{0.05})O_2$, and (c) $Li_y(Ni_{0.475}Mn_{0.475}Al_{0.05})O_2$ charged to 4.3 V. DSC profile of $Li_y(Ni_{0.80}Co_{0.20})O_2$ (dotted lines) charged to 4.2 V was taken from [7] for comparison.

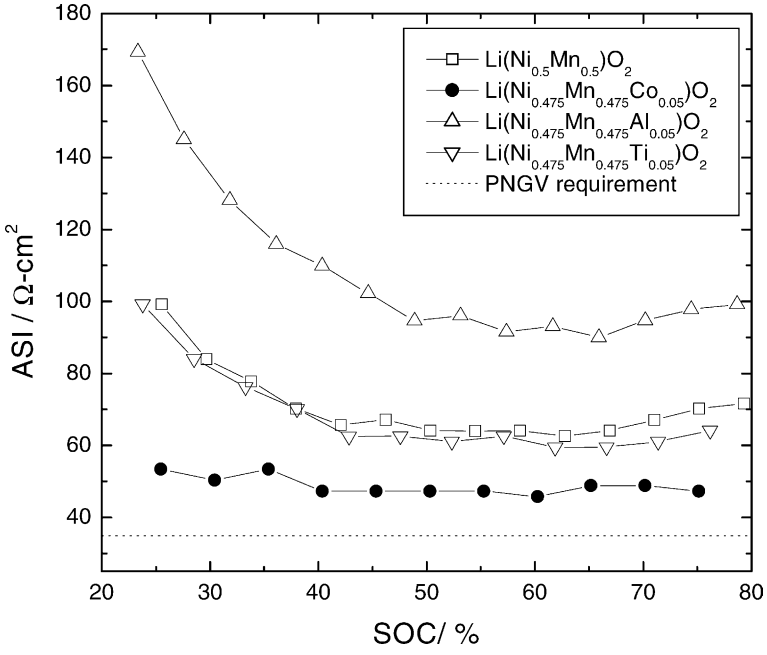

Fig. 7. Area specific impedance (ASI) of C/Li($Mn_{0.475}Ni_{0.475}M'_{0.05}$)$O_2$ cells as a function of state of charge (SOC).

4. Summary and conclusions

Layered Li($Ni_{0.5-x}Mn_{0.5-x}M_{2x}'$) (M′ = Mg, Al, Co, Ni, Ti; $x = 0$, 0.025) materials were synthesized using a manganese–nickel hydroxide precursor. Li($Ni_{0.5}Mn_{0.5}$)O_2 delivered discharge capacities of ca. 120 and 150 mAh/g at 2.8–4.3 and 2.8–4.6 V, respectively, with slight fading. The discharge capacity of the materials increased by 10–30% and cycling stability was improved by doping. Cyclic voltammograms of all of the materials suggested that structural phase transitions are not present during the electrochemical cycling. The CV and XPS data suggested that Ni and Mn are present in Li($Ni_{0.5-x}Mn_{0.5-x}M_{2x}'$) samples as Ni^{2+} and Mn^{4+}, respectively. Differential scanning calorimetry experiments revealed that Li($Ni_{0.5-x}Mn_{0.5-x}M_{2x}'$) has better thermal safety characteristics than $LiNiO_2$-based cathode materials.

In conclusion, Li($Ni_{0.5-x}Mn_{0.5-x}M_{2x}'$) are promising candidates for cathode materials in rechargeable lithium-ion batteries in terms of capacity, stability, and thermal safety. But for the materials to be adopted in high-power applications such as HEVs, the impedance of the materials still needs to be improved to meet PNGV requirements. Extensive studies are underway to reduce the materials' impedance. Success in lowering the ASI of these materials to meet the PNGV power requirement will make those materials very attractive for application in HEV batteries because they are lower in cost and could provide batteries with long calendar life and enhanced safety.

Acknowledgements

This work was supported by the US Department of Energy, Office of Advanced Automotive Technologies, under contract No. W-31-109-ENG-38. The XPS experiments were conducted at the Center for Microanalysis of Materials, University of Illinois; this facility is supported by the US Department of Energy under grant DEFG02-96-ER45439. We acknowledge Dr. D. Abraham (ANL) and Dr. Rick Haasch (UIUC) for their assistance in acquiring and processing the XPS data.

References

[1] T. Ohzuku, Y. Makimura, Chem. Lett. 30 (2001) 744.
[2] Z. Lu, D.D. MacNeil, J.R. Dahn, Electrochem. Solid State Lett. 4 (2001) A191.
[3] W. Li, J.N. Reimers, J.R. Dahn, Solid State Ionics 67 (1993) 123.
[4] J.M. Paulsen, C.L. Thomas, J.R. Dahn, J. Electrochem. Soc. 147 (2000) 861.
[5] M.E. Spahr, P. Novak, B. Schnyder, O. Haas, R. Nespar, J. Electrochem. Soc. 145 (1998) 1113.
[6] T. Eriksson, Ph.D. Thesis, Uppsala University, Uppsala, Sweden, 2001.
[7] C.H. Chen, J. Liu, M.E. Stoll, K. Amine, submitted for publication.
[8] Y. Gao, M.V. Yakovleva, W.B. Ebner, Electrochem. Solid State Lett. 1 (1998) 117.
[9] PNGV Battery Test Manual, Revision 1, Idaho National Engineering Laboratory, Department of Energy, DOE/ID-10597, May 1998.